Astronomy & Astrophysics

Time variation of radial gradients in the Galactic disk: electron temperatures and abundances

W. J. Maciel[1], C. Quireza[2], and R. D. D. Costa[1]

[1] Instituto de Astronomia, Geofísica e Ciências Atmosféricas (IAG/USP), Universidade de São Paulo, Rua do Matão 1226, 05508-900 São Paulo SP, Brazil
e-mail: [maciel;roberto]@astro.iag.usp.br

[2] Observatório Nacional, Rua General José Cristino 77, 20921-400 Rio de Janeiro RJ, Brazil
e-mail: quireza@on.br

ABSTRACT

Aims. We investigate the electron temperature gradient in the galactic disk as measured by young HII regions on the basis of radio recombination lines and the corresponding gradient in planetary nebulae (PN) based on [OIII] electron temperatures. The main goal is to investigate the time evolution of the electron temperature gradient and of the radial abundance gradient, which is essentially a mirror image of the temperature gradient.

Methods. The recently derived electron temperature gradient from radio recombination lines in HII regions is compared with a new determination of the corresponding gradient from planetary nebulae for which the progenitor star ages have been determined.

Results. The newly derived electron temperature gradient for PN with progenitor stars with ages in the $4-5$ Gyr range is much steeper than the corresponding gradient for HII regions. These electron temperature gradients are converted into O/H gradients in order to make comparisons with previous estimates of the flattening rate of the abundance gradient.

Conclusions. It is concluded that the O/H gradient has flattened out in the past 5 Gyr at a rate of about 0.0094 dex kpc^{-1} Gyr^{-1}, in good agreement with our previous estimates.

Key words. ISM: abundances – planetary nebulae: general – Galaxy: abundances – Galaxy: evolution

1. Introduction

Radial abundance gradients in the galactic disk and their time variations are among the main constraints of chemical evolution models for the Milky Way. These gradients can be determined from a variety of objects, such as HII regions, cepheid variables, open clusters and planetary nebulae (PN). In a recent series of papers, Maciel et al. (2003, 2005, 2006) estimated the time variation of the radial abundance gradients taking into account a large sample of PN for which abundances of O/H, S/H, Ne/H and Ar/H have been derived. Based on individual estimates of the progenitor star ages, it was concluded that the radial gradients are flattening out at an average rate of about $0.005-0.010$ dex kpc^{-1} Gyr^{-1} for the last 8 Gyr, approximately. A comparison of the PN gradients with results from HII regions, OB stars and associations, cepheids and, especially, open cluster stars, strongly supports these conclusions.

On the other hand, it has long been known that a positive electron temperature gradient of about $250-450$ K/kpc is observed in the galactic disk, mainly on the basis of radio recombination line work on HII regions (see for example Churchwell & Walmsley 1975; Churchwell et al. 1978; Shaver et al. 1983; Wink et al. 1983; Afflerbach et al. 1996; and Deharveng et al. 2000). Such a gradient is interpreted as a reflection of the radial abundance gradient of elements such as O/H, S/H, etc. in the galactic disk, since these elements are effective coolants of the ionized gas (see for example Shaver et al. 1983).

Recently, Quireza et al. (2006) presented a detailed study of a large sample containing over a hundred HII regions spanning about 17 kpc in galactocentric distances for which accurate electron temperatures were determined from radio recombination lines, specifically H91α and He91α. The observations were made with the 140 Foot telescope of the National Radio Astronomy Observatory (NRAO), and are of unprecedented sensitivity compared with previous studies. According to this work, the best estimate of the gradient, obtained from a sample of 76 sources with high quality data, is $dT_e/dR \simeq 287\pm46$ K/kpc, with no significant variations along the galactocentric distances. A slightly larger gradient (up to 17%) was obtained by excluding some HII regions which are closer to the galactic centre, and may not belong to the disk population.

Regarding planetary nebulae, our earlier work (Maciel & Faúndez-Abans 1985) based on a sample of PN classified according to the Peimbert types (cf. Peimbert 1978) suggested a positive electron temperature gradient in the range $550-800$ K/kpc, somewhat steeper than the HII region gradients observed at the time.

In this work, we take into account the recent PN samples analyzed by Maciel et al. (2003, 2005, 2006) and derive the PN electron temperature gradient for a sample of objects having similar ages. A comparison of the obtained T_e gradient with the recently derived value by Quireza et al. (2006) for HII regions gives then an independent estimate of the time variation of the radial abundance gradients in the galactic disk.
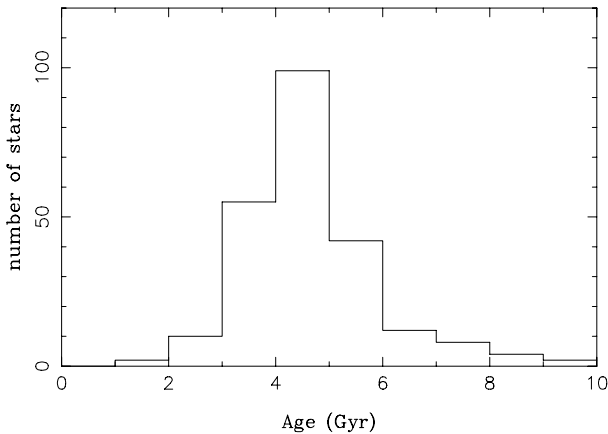
Fig. 1. Age distribution of the PN progenitor stars in the Basic Sample of Maciel et al. (2006).

Fig. 2. Galactocentric variation of the [OIII] electron temperatures for PN with progenitor ages of 4–5 Gyr. The empty circles show some nebulae having extremely hot central stars, not included in the linear regression analysis.

2. The electron temperature gradient in the galactic disk

The determination of abundance gradients is a difficult task, basically for three main reasons. First, the magnitudes of the gradients are small, amounting at most to a few hundredths in units of dex/kpc, so that a relatively large galactocentric baseline is needed in order to obtain meaningful results. Second, the uncertainties both in the abundances and in the distances contribute to the observed scattering, so that large samples are usually needed. Third, chemical evolution models generally predict some time variation of the gradients, so that it is extremely important to take into account in a given sample only objects with similar ages. For these reasons, some of the analyses of gradients in the literature produce relatively flat gradients (see for example Perinotto & Morbidelli 2006). On the other hand, accurate and homogeneous abundances eliminate some of these problems, so that relatively steeper gradients are obtained, as in Pottasch & Bernard-Salas (2006).

In our recent work, we made an attempt to overcome some of these problems, and estimated the individual ages of the PN progenitor stars using an age-metallicity relationship which also depends on the galactocentric distance. As a result, we have obtained the age distribution shown in Fig. 1, adopting our Basic Sample, which is the largest and most complete sample we have considered, containing 234 nebulae (see Maciel et al. 2003, 2005, 2006 for details).

It can be seen that the ages are strongly peaked around 4−5 Gyr, where we have 99 objects. In the present work, we will consider the objects in this age bracket, in order to make comparisons with the younger HII regions. We have then collected the electron temperatures of the planetary nebulae, selecting only the [OIII] temperatures in order to keep our sample as homogenous as possible. These temperatures are determined from the ratio of the [OIII] 4363/5007 Å lines, which are usually among the brightest collisionally excited emission lines in the spectra of planetary nebulae. We have preferred our own data where available (Costa et al. 2004, 1996; see a list of references in Maciel et al. 2003, 2005, 2006), with additional data by Henry et al. (2004), Kingsburgh & Barlow (1994), and Cahn et al. (1992). The resulting T_e variation with galactocentric distance R is shown in Fig. 2, where we adopted the same distances and solar galactocentric radius as in our previous work. The total number of objects in Fig. 2 is somewhat lower than shown in
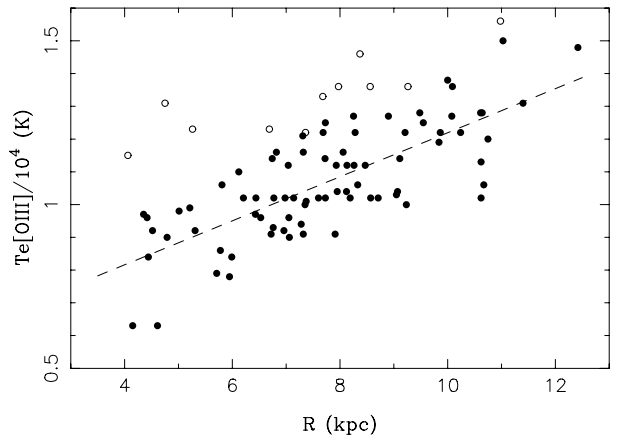
the 4−5 Gyr bracket of Fig. 1, as for a few nebulae we could not obtain accurate electron temperatures.

It can be seen from Fig. 2 that there is a clear tendency in the sense that higher electron temperatures are associated with larger galactocentric distances. The best derived T_e gradient for this sample of PN is $dT_e/dR \simeq 670 \pm 65$ K/kpc, with a correlation coefficient of $r \simeq 0.76$, which is similar to the gradient for the "selected sample" of our earlier paper (Maciel & Faúndez-Abans 1985). Adopting instead a homogeneous set of [OIII] electron temperatures from Henry et al. (2004), which is the largest homogeneous sample available for these nebulae, we obtain essentially the same result, namely $dT_e/dR = 680 \pm 140$ K/kpc and $r \simeq 0.65$, so that the correlation is real. Our best derived slope is illustrated by the dashed line in Fig. 2.

The average uncertainty in the determination of the electron temperatures is generally considered to be within 10% for the brightest nebulae, which corresponds roughly to 1000 K for most objects (see for example Kingsburgh & Barlow 1994; and Krabbe & Copetti 2005). For the galactocentric distances an average uncertainty is more difficult to establish, as it depends on the adopted distances. Since most objects in Fig. 2 are located within about 3 kpc from the solar galactocentric radius, an average error of 50% in the distances would correspond to a shift in the galactocentric distances of about 0.03−1.0 kpc depending on the distance and the direction of the line of sight to the nebula. As a comparison, for the HII regions in the sample by Quireza et al. (2006), average formal uncertainties in the electron temperatures are within 2%, but systematic errors may increase this uncertainty up to 10% for the best data. For spectrophotometric distances, average errors of 15% are quoted, while for kinematic distances non-circular streaming motions may increase this figure to about 25%. From the $T_e \times R$ plot by Quireza et al. (2006), an average dispersion of about 2200 K can be obtained, which is about half the dispersion in Fig. 2.

It should be noted that the dispersion observed in Fig. 2 is probably real, since the electron temperatures may be affected by several factors, such as differences in the effective temperature of the central stars, presence of dust, optical depth effects, electron density and temperature fluctuations, etc., apart from the main cause of the $T_e \times R$ variation, namely, the radial abundance gradient. These effects are also partially responsible for the observed dispersion in HII regions, but for PN the variations in the effective temperatures of the central stars and the
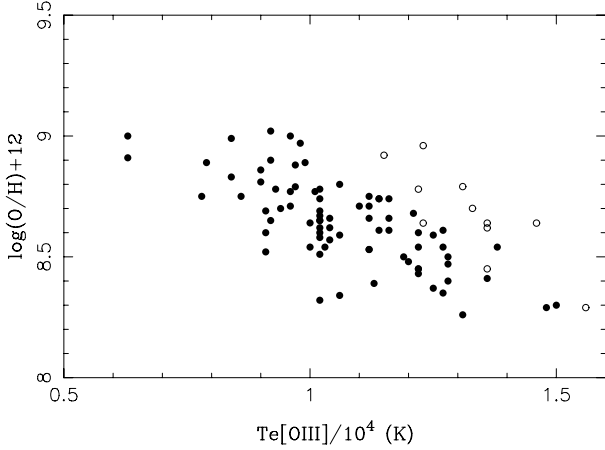
Fig. 3. The inverse correlation between the [OIII] electron temperatures and the O/H abundances for PN in the 4–5 Gyr age bracket. The empty circles show some nebulae having extremely hot central stars.

uncertainties in the distances are larger, so that the observed dispersion in Fig. 2 is larger than in the case of HII regions. As a consequence, some nebulae appear not to follow the observed correlation very closely. In particular, PN having extremely hot central stars, with temperatures in excess of 10^5 K, generally have higher electron temperatures than expected by their galactocentric distances. Furthermore, these objects come from more massive progenitors than most nebulae, so that their ages may be lower than $4-5$ Gyr, as assumed. Some examples include M1-57, Me2-1, PB6, NGC 6620 and a few others, which are plotted in the figure as empty circles. Other objects with hot central stars, such as NGC 2899, NGC 6302, NGC 6537 and NGC 7008 are not plotted in Fig. 2, as their electron temperatures are too high to fit the scale. All these nebulae have not been included in the linear regression, so that our derived electron temperature gradient applies to stars with temperatures lower than 10^5 K. In this analysis we have used Zanstra temperatures and energy-balance temperatures (see for example Preite-Martinez et al. 1991; Méndez et al. 1992; Zhang 1993; and Stasińska et al. 1997).

Another interesting object is M1-9, which is the nebula with the largest galactocentric distance in the sample ($R \simeq 12.4$ kpc). In view of its position on the $T_e \times R$ plane, it may single-handedly affect the derived slope. For this object, our own results suggest an electron temperature of $T_e \simeq 11\,000$ K (Costa et al. 1996), but a more detailed study by Tamura & Shibata (1990) and Shibata & Tamura (1985) gives a larger value, $T_e \simeq 14\,800$ K, which is adopted here. This object may then alter the derived slope by about 50 K/kpc, but the main conclusions of this paper are unaffected.

The association of higher electron temperatures with lower metallicities can be seen from Fig. 3, where we show the inverse correlation between the [OIII] electron temperatures and the O/H abundances for the objects with ages in the $4-5$ Gyr bracket. PN with central stars hotter than 10^5 K are also shown as empty circles. Again a relatively large dispersion is observed, but the inverse correlation is clear, confirming that oxygen is among the main coolants in the photoionized gas within the planetary nebulae.

3. Comparison of the PN and HII gradients

From a straigthforward comparison of the electron temperature gradient for PN and HII regions we can already conclude that

there is some flattening of the gradients during the time interval of about 5 Gyr, which is essentially the difference between the ages of the PN progenitor stars considered in this work and the much younger HII regions in the sample by Quireza et al. (2006). In other words, the conclusions of our recent series of papers are supported by the obtained differences between the electron temperature gradients of PN and HII regions, in view of the fact that these gradients essentially reflect the radial abundance gradients in the galactic disk. In order to make a direct comparison with the estimated flattening rate of the abundance gradients derived by Maciel et al. (2005), we can convert the T_e gradient into the equivalent O/H gradient. For HII regions we can use the calibration by Shaver et al. (1983), according to which the oxygen gradient is related to the electron temperature gradient by

$$\frac{\mathrm{d}\log(\mathrm{O/H})}{\mathrm{d}R} \simeq -1.49 \times 10^{-4} \frac{\mathrm{d}T_e}{\mathrm{d}R} \tag{1}$$

where the temperature gradient is in K/kpc and the oxygen gradient is in dex/kpc. This relation is also supported by more recent work on HII regions, such as the analysis by Deharveng et al. (2000). The oxygen gradient for HII regions is then $\mathrm{d}\log(\mathrm{O/H})/\mathrm{d}R \simeq -0.043$ dex/kpc, which is similar to the value obtained by Deharveng et al. (2000) based on an entirely different sample. Also, an O/H gradient of -0.044 dex/kpc was recently obtained by Esteban et al. (2005) from oxygen recombination lines, a method almost independent of the assumed electron temperatures, and totally independent of the [OIII] forbidden lines. A similar estimate has been presented by Quireza et al. (2006), also based on the Shaver et al. (1983) calibration.

For planetary nebulae, we can have an idea of the corresponding O/H gradient by inspecting Table 1 of Maciel et al. (2005) for Group II objects (ages of 4–5 Gyr), from which we get dlog(O/H)/d$R \simeq -0.089 \pm 0.003$ dex/kpc. Alternatively, we can compute the O/H gradient directly for the PN sample adopted here, in which case we get a similar value, $\mathrm{d}\log(\mathrm{O/H})/\mathrm{d}R \simeq -0.090$ dex/kpc. Therefore, the flattening rate of the oxygen gradient can be estimated by

$$\chi \simeq \frac{1}{\Delta T} \left[\frac{\mathrm{d}\log(\mathrm{O/H})}{\mathrm{d}R} \bigg|_{\mathrm{HII}} - \frac{\mathrm{d}\log(\mathrm{O/H})}{\mathrm{d}R} \bigg|_{\mathrm{PN}} \right] \tag{2}$$

so that $\chi \simeq 0.0094$ dex kpc^{-1} Gyr^{-1} where we have used $\Delta t \simeq 5$ Gyr. In view of our discussion on the electron temperatures of planetary nebulae, we would expect the rate to be somewhat smaller than this value, which is in excellent agreement with the range estimated by Maciel et al. (2005), namely $\chi \simeq 0.005-0.010$ dex kpc^{-1} Gyr^{-1}.

As mentioned in the introduction, abundance gradients and their time variation are valuable constraints for chemical evolution models. As an illustration, we have compared our derived flattening rate with the predictions of some recently published models for the Milky Way. As discussed by Maciel et al. (2006) there may be large discrepancies between different chemical evolution models, even whithin the so-called "inside-out" class of models. In particular, Hou et al. (2000) adopted an exponentially decreasing infall rate for the galactic disk, in which a rapid increase in the metal abundance at early times in the inner disk leads to a steep gradient. As times goes on, the star formation migrates to the outer disk and metal abundances are enhanced in that region, with the consequence that the gradients flatten out. A rough estimate for the O/H gradient variation in these models leads to a steepening rate of $\chi \simeq 0.0040-0.0060$ dex kpc^{-1} Gyr^{-1}, which is consistent with our present results. A similar behaviour has also been obtained

by Alibés et al. (2001). On the other hand, models such as those based on two infall episodes by Chiappini et al. (2001), lead to some steepening of the gradients, even though the inside-out approach is adopted. Possibly, the main reason for the different predictions of the quoted models appears to reside on the different adopted timescales for star formation and infall rate, so that we expect our present results may be helpful in order to constrain these quantities.

References

Afflerbach, A., Churchwell, E., Acord, J. M., et al. 1996, ApJS, 106, 423
Alibés, A., Labay, J., & Canal, R. 2001, A&A, 370, 1103
Cahn, J. H., Kaler, J. B., & Stanghellini, L. 1992, A&AS, 94, 399
Chiappini, C., Matteucci, F., & Romano, D. 2001, ApJ, 554, 1044
Churchwell, E., & Walmsley, C. M. 1975, A&A, 38, 451
Churchwell, E., Smith, L. F., Mathis, J., Mezger, P. G., & Huchtmeier, W. 1978, A&A, 70, 719
Costa, R. D. D., Chiappini, C., Maciel, W. J., & de Freitas Pacheco, J. A. 1996, A&AS, 116, 249
Costa, R. D. D., Uchida, M. M. M., & Maciel, W. J. 2004, A&A, 423, 199
Deharveng, L., Peña, M., Caplan, J., & Costero, R. 2000, MNRAS, 311, 329
Esteban, C., García-Rojas, J., Peimbert, M., et al. 2005, ApJ, 618, L95
Henry, R. B. C., Kwitter, K. B., & Balick, B. 2004, AJ, 127, 2284
Hou, J. L., Prantzos, N., & Boissier, S. 2000, A&A, 362, 921
Kingsburgh, R. L., & Barlow, M. J. 1994, MNRAS, 271, 1994
Krabbe, A. C., & Copetti, M. V. F. 2005, A&A, 443, 981
Maciel, W. J., Costa, R. D. D., & Uchida, M. M. M. 2003, A&A, 397, 667
Maciel, W. J., & Faúndez-Abans, M. 1985, A&A, 149, 365
Maciel, W. J., Lago, L. G., & Costa, R. D. D. 2005, A&A, 433, 127
Maciel, W. J., Lago, L. G., & Costa, R. D. D. 2006, A&A, 453, 587
Méndez, R. H., Kudritzki, R. P., & Herrero, A. 1992, A&A, 260, 329
Peimbert, M. 1978, Planetary Nebulae, ed. Y. Terzian (Dordrecht: Reidel), IAU Symp., 76, 215
Pottasch, S. R., & Bernard-Salas, J. 2006, A&A, 457, 189
Perinotto, M., & Morbidelli, L. 2006, MNRAS, 372, 45
Preite-Martinez, A., Acker, A., Köppen, J., & Stenholm, B. 1991, A&AS, 88,121
Quireza, C., Rood, R. T., Bania, T. M., Balser, D. S., & Maciel, W. J. 2006, ApJ, 653, 1226
Shaver, P. A., McGee, R. X., Newton, L. M., Danks, A. C., & Pottasch, S. R. 1983, MNRAS, 204, 53
Shibata, K., & Tamura, S. 1985, PASJ, 37, 325
Stasińska, G., Górny, S. K., & Tylenda, R. 1997, A&A, 327, 736
Tamura, S., & Shibata, K. 1990, PASJ, 102, 1301
Wink, J. E., Wilson, T. L., & Bieging, J. H. 1983, A&A, 127, 211
Zhang, C. Y. 1993, ApJ, 410, 239